Combined effect of ignition and injection timing along with hydrogen enrichment to natural gas in a direct injection engine on performance and exhaust emission

J* Zareei, A.Rohani, Wan Mohd[2]

1-Department of Bio Systems Engineering, Faculty of Agriculture, Ferdowsi University of Mashhad, Mashhad, Iran

2- Department of Mechanical & Materials Engineering, national university of Malaysiamasih@iust.ac.ir

Abstract

To improve the engine performance and reduce emissions, factors such as changing ignition and injection timing along with converting of port injection system to direct injection in SI(spark-ignited) engines and hydrogen enrichment to CNG fuel at WOT conditions have a great importance. In this work, which was investigated experimentally (for CNG engine) and theoretically (for combustion Eddy Break-Up model and turbulence model is used) in a single- cylinder four-stroke SI engine at various engine speeds (2000-6000 rpm in 1000 rpm intervals), injection timing (130-210 crank angle(CA) in 50 CA intervals), ignition timing (19-28 CA in 2 degree intervals), 20 bar injection pressure and five hydrogen volume fraction 0% to 50% in the blend of HCNG. The results showed that fuel conversion efficiency, torque and power output were increased, while duration of heat release rate was shortened and found to be advanced. NOx emission was increased with the increase of hydrogen addition in the blend and the lowest NOx was obtained at the lowest speed and retarded ignition timing, hence 19° before top dead center.

***Keywords**: HCNG Fuel; Ignition and Injection Timing; Performance and Emissions*

1. Introduction

In the recent years, the issue of energy conservation and environmental protection has become increasingly important, thus for improving thermal efficiency and emissions performance in internal combustion engines, hydrogen fuel is considered as a renewable energy due to its high flame speed, low ignition energy, and wide flammable range [1-3]. Cycle-to-cycle variation in port injection engines with fueled natural gas becomes an urgent problem because of long combustion duration in SI engine [4-6]. The increase a small amount of methane in direct injection engine is very similar to lean limit extension using hydrogen addition [7-10]. By using hydrogen in the blend of HCNG between 10 and 34%, showed that engine brake efficiency and power output at a different percent of hydrogen have a positive effect and increasingly [11]. Also, cycle-by-cycle variations as a result of an increase of 10 percent hydrogen by Yu et al., showed that with various excess air ratio and throttle position, coefficient of variation in indicated mean effective pressure decreased firstly and increased afterward with the retard in ignition timing[12]. Adding hydrogen or natural gas in direct injection engine at low load heat release reduced on the combustion of heavy duty diesel engine and experimentally investigated that spark timing(32° b TDC) increase pressure peak and decrease maximum brake torque in HCNG blend engine [13, 14]. In the experimental results by Xin et al., from 15% to 35% in volume can find that the engine work stability is largely improved with the higher hydrogen fraction [15]. NOx emission increased when enriching H2 so that reduction of CO and CO2 are observed [16-19]. Hydrogen/ methane mixtures have been considered by Zaker. et al., using an open cycle Computational Fluid Dynamics (CFD) simulation [20]. 20-30 percent excessive air does not affect NOx levels considerably, but at maximum brake torque condition, all fuel is consumed to 10 degrees after TDC and maximum CO at this point transmute to CO2 afterwards [20-22].

In this study, the engine performance and emissions of hydrogen and natural gas blend fuel examined in a four-stroke spark ignition engine with direct fuel injection. Simulation and Experiments were conducted at constant load of WOT as engine speed ranging from 2000 to 6000 rpm. The simulation and

[DOI: 10.22068/ijae.8.1.2614]

experimental results were compared with that of pure CNG. In-cylinder pressure, engine output torque, fuel consumption as well as regulated gas emissions (CO, NOX) were mainly obtained and analyzed by using AVL Fire software. In the following sections, simulation and modeling procedure are explained, and then results are discussed. Finally, major conclusions are summarized in the last section.

2. Geometry and grid generation of engine and operating condition

As showed in Fig. 1(a) typical CNGDI engine with a single cylinder and two exhaust and intake valves is used. In this engine are used two different shapes of the piston that is applied for examining pattern and behavior of turbulence tumble and swirl intensity field inside the cylinder to obtain suitable piston shape for the combustion process. To verifying the suitable piston crown for the analysis of heat transfer and turbulence characteristic and preparation of fuel mixing for the subsequent best combustion process, two different piston shapes were examined. A bowl was positioned at the center of piston a crown. Surface mesh generation is done on CAD program. After that, surface data was converted into the finite volume mesh in order to deal with the CFD analysis. A grid generator program was used to generate hexahedral cells for the CFD calculation of computational mesh. In the CFD calculation, finite volume method is used. Mesh in 3D models which includes nodes, faces and volumes and numerical values for desired quantities in node positions are calculated.

3. Ignition Modelling

In this work, one objective is to account for exhaust emissions related to hydrogen enrichment. Consequently, two kinds of ignition must be modelled: The spark ignition (AKTIM model), the auto-ignition at the origin of knock phenomenon. Those models are embedded in an ECFM3Z model framework. This last is used for the modelling of classical combustion processes (diffusion or propagation flame, using a dedicated laminar flame speed correlation). The first step of the present computational study was to find a laminar flame speed correlation which will be well suited to represent the combined combustion of methane and hydrogen for various volume ratios. Most correlations for the combustion of light hydrocarbons are mostly based on the one first developed by Methgalchi and Keck for the mixture of air with propane, methanol, isooctane or indolence[23].

4. Fuel chemical equation and engine specifications

The fuel is introduced in the combustion chamber and mixed with air. The chemical equation of the process is:

$$\varepsilon.\phi\left(v_1 CH_4(g)+v_2 H_2(g)\right)_{(T_f P_f)}+\left(0.21O_2+0.79N_2+\varpi H_2O\right)_{(T_i,P_i)}$$
$$\rightarrow\left(0.21O_2+0.79N_2+\varpi H_2O\right)_{(T,P)}+\varepsilon.\phi.\left(v_1 CH_4(g)+v_2 H_2(g)\right)_{(T,P)}$$

Where ε is the total mole number of fuel, ϕ represents the fuel/air equivalence ratio, ϖ represents the molar humidity ratio, and v_i stands for the mole amount of component i per mole of fuel mixture. If pure natural gas is used, $v_2=0$, but $v_1=0$ if pure hydrogen is used.

The chemical formulas for combustion of stoichiometric hydrogen–air and methane–air mixture are as follows:

$$CH_4+2(O_2+3.76N_2)=CO_2+2H_2O+2\times3.76N_2$$

$$H_2+0.5(O_2+3.76N_2)=H_2O+0.5\times3.762N_2$$

The engine operating conditions for the baseline condition of CFD simulation were chosen at a fixed speed at 2000, 3000, 4000, 5000 and 6000 rpm. The investigated engine operating conditions covered certain variations in the intake temperature, injection timing, injection duration, and spark ignition timing. The obtained engine operating conditions from the experimental data of single cylinder research engine (SCRE) are listed in Table 1.

Fig. 1. the computational domain of the engine model

[DOI: 10.22068/ijae.8.1.2614]

Table 1. Specification of the CNG-DI engine

Engine parameter	Value	Unit	Engine parameter	Value	Unit
Maximum rated power (kW/rpm)	82/6000	kW/rpm	Intake valve opening	12	bTDC
Maximum rated torque (Nm/rpm)	148/4000	Nm/rpm	Intake valve closing	48	aBDC
Stroke	84	mm	Exhaust valve opening	45	bBDC
Connecting rod length	131	mm	Exhaust valve closing	10	aTDC
Crank radius	44	mm	Maximum intake valve lift	8.1	Mm
Compression ratio	14	-	Maximum exhaust valve lift	7.5	Mm
Fuel			CNG+ Hydrogen		

Table 2. Baseline Engine Operating Conditions

Engine Parameters and Unit	Value				
Engine Speed (rpm)	2000	3000	4000	5000	6000
CNG mass(mg)	5.2	5.2	5.2	5.2	5.2
Equivalence Ratio	1.0	1.0	1.0	1.0	1.0
Intake Port Temperature (K)	305	305	305	305	306
Intake Port Pressure (bar)	1.04	1.03	1.02	1.01	0.9
Start of Injection Timing (bTDC)	130	150	170	190	210
End of Injection Timing (bTDC)	80	100	120	140	160
Spark Ignition Timing (bTDC)	19	21	23	25	28
Injection pressure(bar)	20	20	20	20	20

The CFD simulation was executed by defining the events for engine cycle and it is started from the crank angle degree of 0ºCA by defining the value of initial pressure and temperature. The simulation finished at the crank angle degree of top dead center, where the exhaust valves will be opening. The measured intake temperature from the experimental work has been implemented to the engine computational mesh, as the piezo static pressure boundary condition. Injection and ignition timings were adjusted appropriately according to increasing engine speeds. Engine operating conditions are shown in Table 2.

Table 3. Shows the energy and mass composition of each type of fuel used in the investigation. Also, Table 4 show some Properties of hydrogen and methane (nearly to natural gas properties) fuel under stoichiometric condition.

For calculating the amount of table 3 should be solved the equation of combustion.

5. Solution algorithm

In order to attain the best compromise between the computing load and convergence requirements, it is necessary to define the time discretization that is, for simulations initiation the smaller time steps are positioned as well as around the TDC and fuel injection position. Time steps for engine speeds are as the table below:

Time step for (2000 rpm) and (6000 rpm) was different and were defined as 8.3 µs and 2.7 µs and its amount for 3000, 4000 and 5000 rpm was equal with 6.9, 4.5 and 3.1 µs respectively. To meet the unconditional numerical stability, the temporal discretisation is implicit and the under relaxation factors are 0.3. While the accurate second order differencing scheme of MARS (monotone advection and reconstruction scheme) is employed for the

[DOI: 10.22068/ijae.8.1.2614]

momentum, energy and turbulence equations together with the arbitrary Lagrangian Eulerian technique to treat the grid movement associated with the moving of piston and valves. The popular PISO algorithm for unsteady flows is then carried out to solve the resulting algebraic equations. The complexity of the fluid motion in a cylinder illustrates the difficulties involved in investigating the movement and behaviour of combustion inside a cylinder of an engine. Thus, the theoretical study of the effects of engine parameters on performance and emissions of a natural gas-fueled engine is quite a task. The basic philosophy of the model is shown as a flow diagram in Figure 2.

6. Validation of the model using experimental results

The most popular technique for validation is using experimental results due to the fact that the measurement shows the consistency of the model with the reality. To validate the results of the simulation, it is essential to achieve the highest similarity between the measurement and simulation configurations. The most important issue is for the computing environment (simulation) one should try to model the entire possible setup or at least, include the most important characteristics. Otherwise, it runs the risk that the simulation results do not represent the reality faithfully, causing a validation error. For this study, the experimental results of constant volume combustion bomb (CVCB) provided by Tinaut et al., under given operating conditions, have been used to validate the model [25]. Therefore, the operating conditions imposed in this study have been used; the experimental result used for validation purposes is pressure and the specifications of the constant volume combustion bomb used by Tinaut et al., [26]. Table 6 shows the specifications of the cylinder simulated in this work. The designed model for validation purposes is shown in Fig. 3.

Table 3. Energy and Mass Composition of H_2-NG fuel

	CNG	HCNG10	HCNG20	HCNG30	HCNG40	HCNG50
H_2(% Mass)	0	1.21	2.69	4.52	6.72	9.02
H_2(% energy)	0	3.09	6.68	10.49	15.59	20.93
LHV(MJ/Kg)	46.28	47.17	48.26	49.61	51.41	53.294
LHV stoich. mixture(MJ/NM^3)	3.376	3.359	3.353	3.349	3.344	3.340
CNG mass(mg)	5.2	5.13708	5.06012	4.96496	4.855	4.7474
Hydrogen mass(mg)	0	0.06292	0.13988	0.23504	0.3450	0.4526

Table 4. Properties of hydrogen and methane fuel under stoichiometric condition[24]

Properties	Hydrogen	Methane	Unit
Flammability limits	4–75	5–15	Vol. %
Minimum ignition energy	0.02	0.29	mJ
Flame temperature	2045	1875	℃
Auto ignition temperature	585	540	℃
Diffusion coefficient	0.61	0.20	10^{-3} m2/s
Maximum velocity of flame	3.46	0.43	m/s
Density	0.65	0.08	kg/m^3

[DOI: 10.22068/ijae.8.1.2614]

Table 5. The amount of time steps at different speeds

Engine speed (rpm)	2000	3000	4000	5000	6000
Time steps (μs)	8.3	6.9	4.5	3.1	2.7

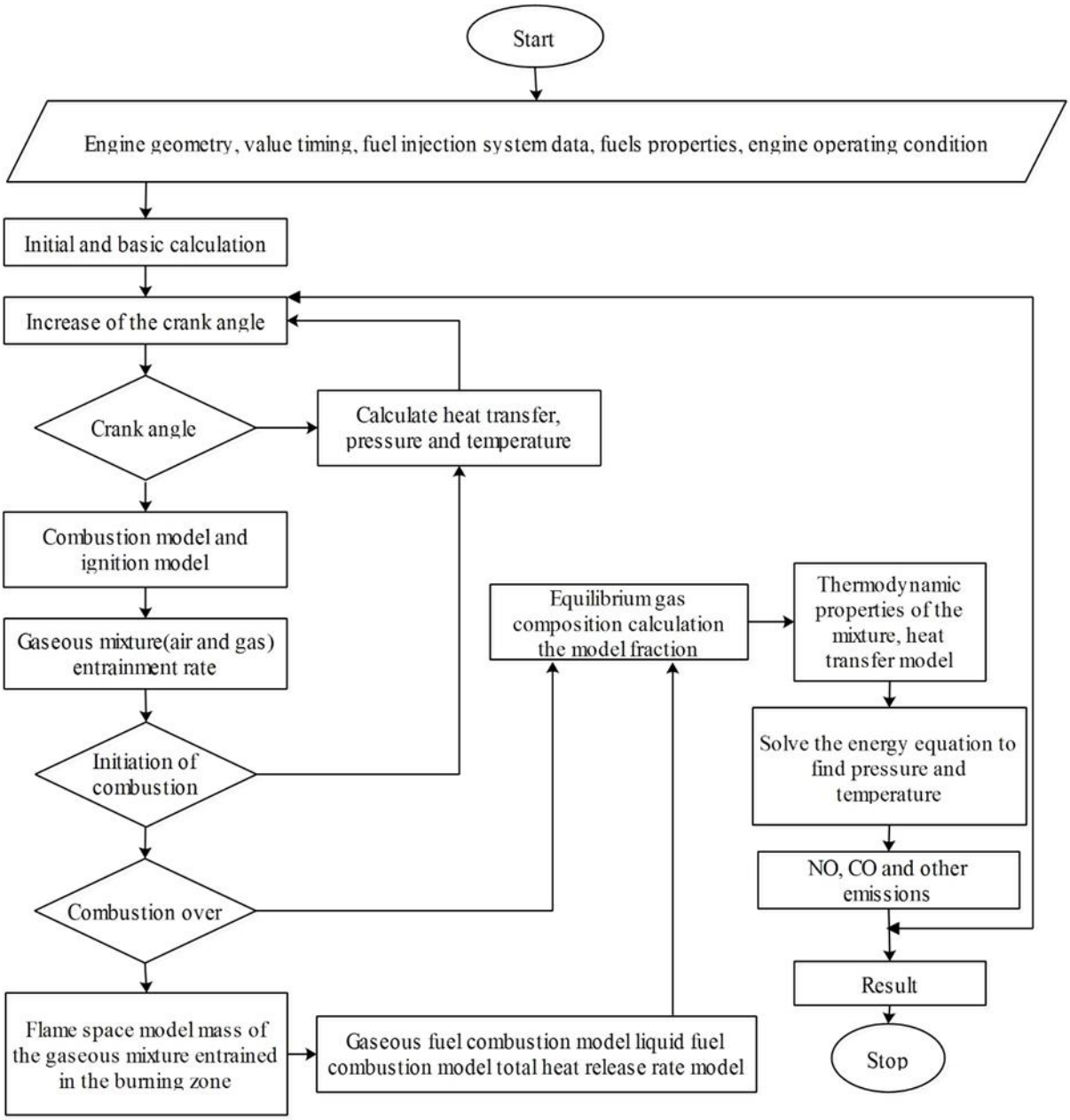

Fig.2. the flow chart of the combustion model

[DOI: 10.22068/ijae.8.1.2614]

Figure 4 shows the evolution of pressure as a function of time for validation between experimental by Tinaut et al., and calculated data from simulation in this study [25]. Some parameters of the actual cylinder are unknown and have been adjusted to obtain the best approximation effect. Calculating error allows comparing an estimate to an exact value. The RMSE and MAPE give the difference between the approximate and exact values and can help to see how close experimental data or estimate was to a real value.

$$MAPE = \frac{1}{n}\sum_{i=1}^{n}\left|\frac{y_{e_i} - y_{s_i}}{y_{e_i}}\right| \times 100 \quad (4)$$

$$RMSE = \sqrt{\frac{\sum_{i=1}^{n}(y_{e_i} - y_{s_i})^2}{n}} \quad (5)$$

Where, ys and ye are simulation and experimental value, respectively.

So, with using of above formula and experimental and simulation data, the percentage error is as below tables.

Table 7 show the difference between experimental and calculated data and also figure 4-36 show percentage error in graph form. The results show that the model fits the experimental pressure data with an error lower than 7.6%. Thus it is acceptable for validation of software [27, 28]. Hogg and Ledolter demonstrated that 8.23% error in calculation has a good agreement in evaluation and validation between experiment and numerical models [28].

This experimental validation using CVCB is a reasonable method to validate the simulation results carried out in the present study as the meshing procedures and sub-models used in CNG-DI engine combustion simulation were also used in the CVCB combustion simulation. As the validation was done for 100% natural gas combustion as well as different blends of hydrogen-natural gas in CVCB, the results of hydrogen-natural gas blends in CNG-DI engine in the next chapter can also be safely considered validated.

Table 6. Engine characteristics for model validation of this work

Cylinder parameters	Unit
Spherical cavity diameter	0.2 m
Cylinder resistance to pressure	40 MPa
Cylinder resistance to temperature	1073 K
Injection pressure	20 bar

Fig.3. Schematic of a constant volume combustion bomb for validation with experimental result.

[DOI: 10.22068/ijae.8.1.2614]

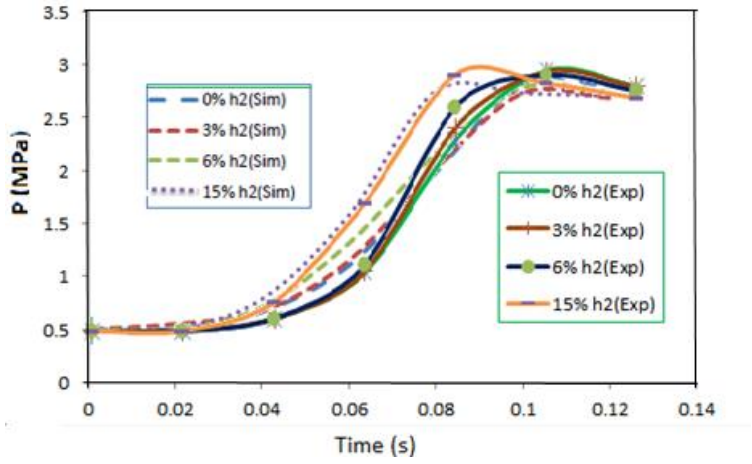

Fig. 4. Curve of cylinder pressure versus time after ignition with the percentage of hydrogen in natural gas (comparison of experimental and simulation data)

Table 7. The value of error based on percentage hydrogen in fuel

	Percentage of hydrogen in blend			
	0	3	6	15
RMSE	0.59	0.53	0.54	0.38
MAPE(%)	13.25	10.42	10.95	6.35

7. Results and discussions

The purpose of this study is to numerically analyses the performance and the pollutant emissions of a four-stroke spark ignition engine operating on natural gas–hydrogen blends of 0%, 10%, 20%, 30%, 40% and 50% hydrogen by volume at full load at 2000, 3000, 4000, 5000 and 6000 rpm engine speeds.

7.1. Influence of Mixtures of Hydrogen and Compressed Natural Gas on Pressure, Temperature and Heat Release Rate in a Direct Injection Engine

Effects of hydrogen and natural gas fuels on the engine performance in terms of maximum in-cylinder pressure, temperature and heat release rate are shown in the following figures. Figure 5 present curves of the cylinder pressure as the function of the CA with HCNG percentages and various spark timings at 2000 to 6000 rpm. Also, Figure 6 shows the start of injection (SOI), and ignition points (figure 6(a,b,c,d,e). The maximum in-cylinder pressure for the mixture of Hydrogen and CNG fuel are higher than that for natural gas fuel vehicles [21]. Hydrogen's fast combustion velocity advanced timing when the maximum in-cylinder pressure occurred while this phenomenon became less obvious in lean burn condition. The peak cylinder pressure increased and appeared with the advancement of CAs and with the addition of increasing amounts of hydrogen. In particular, for 50% hydrogen, the peak cylinder pressure was increased by approximately 9 bars compared with that for 0% hydrogen at 2000 rpm. The peak appeared at an advanced CA, that is, approximately 11 °CA close to the TDC and 8 °CA after the TDC. As shown in Figure below when hydrogen addition to natural gas is increased, (the maximum peak pressure values are found to be close

[DOI: 10.22068/ijae.8.1.2614]

to the TDC). The maximum peak pressure values are obtained at an engine speed of 6000 rpm. Generally, the highest engine efficiency is when maximum pressure occurs at after top dead center [29]. So, spark timing should be regarded as hydrogen fraction increases. Retarding spark timing can not only reduce minus work in compression stroke but also decrease combustion temperature which is good for reducing NOx emission.

Figure 6 presents the maximum temperature of both fuels (hydrogen and natural gas) versus crank angle. The increase of temperature was advanced with changing fuel from CNG to hydrogen. This phenomenon is more obvious when fuel was pure hydrogen since enhancement of burning velocity was more obvious by hydrogen. Also, the in-cylinder temperature increased because of the high adiabatic flame temperature. For 50% hydrogen, the maximum values for in-cylinder temperature and heat release rate were advanced by approximately 10 °CA compared with the corresponding CA for 0% hydrogen. The maximum temperature difference between the 0% H2 and 50% H2 cases was approximately 300 K because the laminar flame speed of a natural gas and hydrogen blend increases with hydrogen addition for a fixed excess air ratio. Cylinder temperature is strongly related to engine thermal efficiency and NOx emissions significantly depend on to combustion temperature [30]. This finding implies that increased heat release and in-cylinder temperature could result in significantly increased NOx emissions with the addition of hydrogen. In Figure 5(a, b, c, d, e) and 6(a, b, c, d and e) is observable that with increasing hydrogen, changes in pressure and temperature are aligned. Therefore the increase of pressure causes that temperature goes up and advanced the maximum temperature. The minimum temperature relates to 0% hydrogen and maximum temperature relates to 50% hydrogen in each engine speed. Minimum temperature is for 0% at 2000 rpm and its maximum is 50% at 6000 rpm.

The heat release rate is defined as the rate at which the chemical energy of the fuel is released by the combustion process. This rate is calculated from the cylinder pressure versus CA as the energy release required creating the measured pressure. From the simulation results, the rate of heat release is directly extracted from the reactive species and their heat formation. By evaluating the heat release rate produced from the engine, the combustion duration can be predicted to maximize the work done when the piston reaches the constant volume stage at the BDC position. Based on the theory of combustion, combustion depends on the equivalence ratio, residual fraction, spark timing, laminar flame speed, turbulence intensity of flow, and combustion chamber shape [31]. Therefore, an increase in hydrogen means an increase in carbon dioxide, an inert gas with large heat capacity, and a decrease in the heating value of the fuel. The engine simulation and modelling for the combustion process of CNG-DI engine by using the multi-dimensional CFD code is very helpful because of its capability to determine the heat release rate occurring within the engine cylinder. The heat release rate generated during the combustion process can be shown in J/deg. As expected in a spark ignition engine, the single peak shape of the heat release profile observed at the same crank angle producing peak pressure. For CNG fuel only, the peak value of around 8.5 J/deg at 2000 rpm occurs during the un premixed combustion phase which is as the result of the rapid combustion of the portion of the injected fuel that has mixed with the air during the ignition delay period. The heat release rate during this phase is also influenced by the injected duration. As the injection duration is increased, the amount of fuel injected increases, thus increasing the magnitude and duration of the mixing controlled heat release. After reaching the maximum value, the heat release decreases during the expansion stroke with random fluctuations due to the incomplete combustion. This is due to the residual fuel burns at the certain region around engine cylinder where the partial combustion occurs and hence deteriorates the combustion efficiency.

The heat release rate for CNG fuel at 6000 rpm engine speed is presented in below figure with its maximum value of 17.137 J/°CA and occurs at 359.5 º CA. After reaching its peak value, the heat release rate decreases to the value of 0.046 J/degree before the exhaust stroke starts. The decrement of heat release rate also depends on the engine speed. The higher mean piston velocity causes the faster heat loss to the cylinder walls.

Figure 7(a, b, c, d, e) shows the heat release rate versus of the CA at different engine speeds. With the addition of hydrogen to NG, the peak heat release rates increased, and the CAs at which they appeared were advanced. Peak heat release was found to be 23.5 J/deg for 50% at 6000 rpm and 8.2 J/deg for 0% at 2000 rpm. Also, the investigation [30]. Mohammed on the heat release rate show that its behavior is similar characteristics to the cylinder pressure [32]. For the case of late injection timing, the cylinder pressure and the heat release rate are observed to be low mainly due to improper air-fuel mixing and the slow combustion rate. With the increase of engine speed, as shown in figures below, when the hydrogen fraction goes up, the heat release rate shows a gradual increase. At low engine speed and high engine load, a similar behavior is presented in the heat release rate, but their amounts

[DOI: 10.22068/ijae.8.1.2614]

are different. One of the important phases in internal combustion engines for different behavior heat release rate is combustion timing and excess air ratio. Thus suggested that combustion at decreased excess air ratio (mixture enrichment) can decrease the combustion difference among mixtures of various hydrogen fractions. The start of injection timing in this study for 2000, 3000, 4000, 5000 and 6000 rpm are 130, 150, 170, 190 and 210 before top dead center respectively. These means that start of injection is constant for each engine speed and should be cleared by the user in AVL fire software.

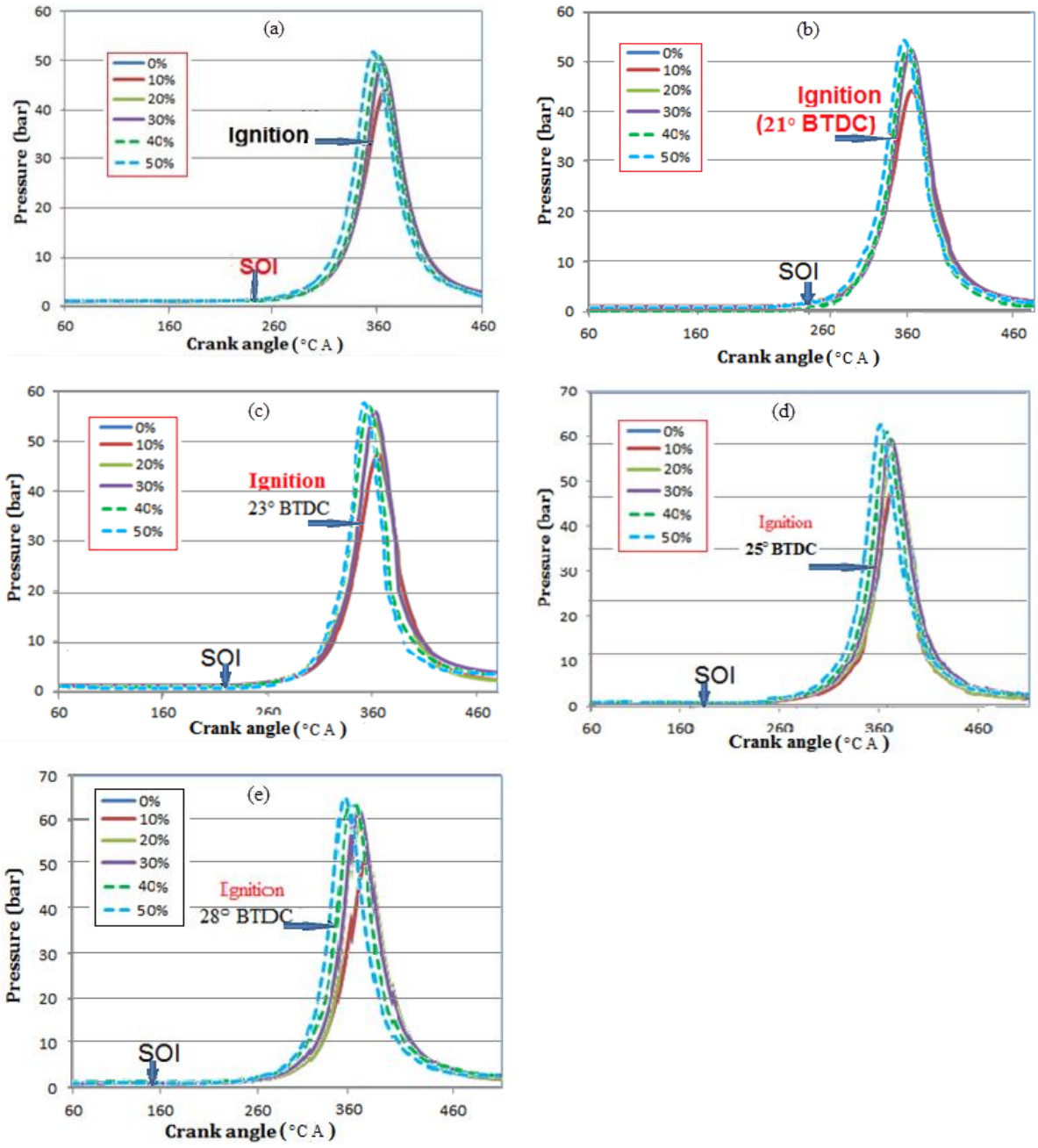

Fig.5. Cylinder pressure as function of the CA with different percentage of hydrogen and spark timing of 19 °CA BTDC at 2000 rpm (a), 21 °CA BTDC at 3000 rpm (b), 23 °CA BTDC at 4000 rpm (c), 25 °CA BTDC at 5000 rpm(d), 28 °CA BTDC at 6000 rpm (e).

[DOI: 10.22068/ijae.8.1.2614]

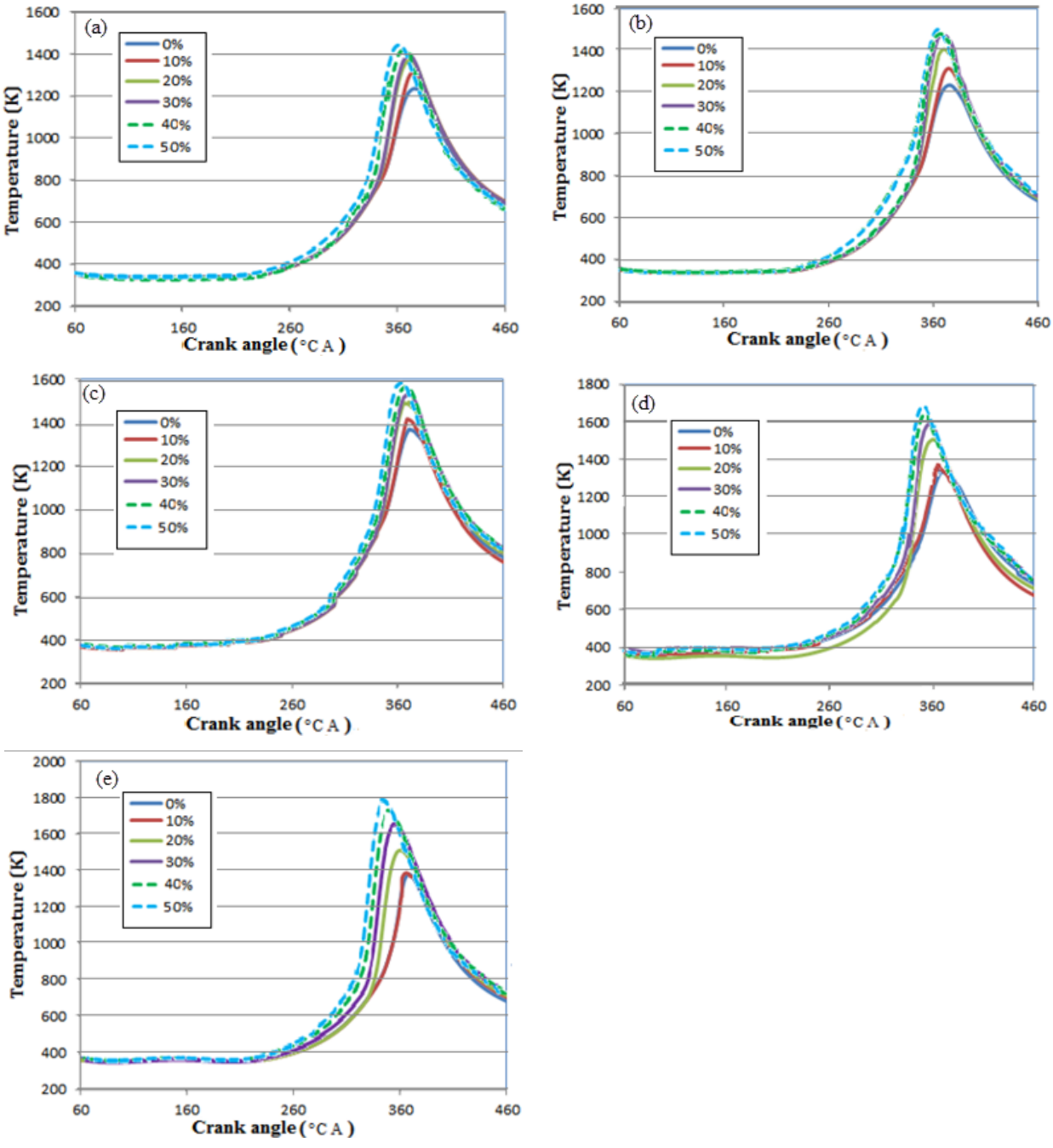

Fig 6. Cylinder temperatures versus the CA with different percentage of hydrogen and spark timing of 19 °CA BTDC at 2000 rpm (a), 21 °CA BTDC at 3000 rpm (b), 23 °CA BTDC at 4000 rpm (c), 25 °CA BTDC at 5000 rpm (d), 28 °CA BTDC at 6000 rpm (e)

[DOI: 10.22068/ijae.8.1.2614]

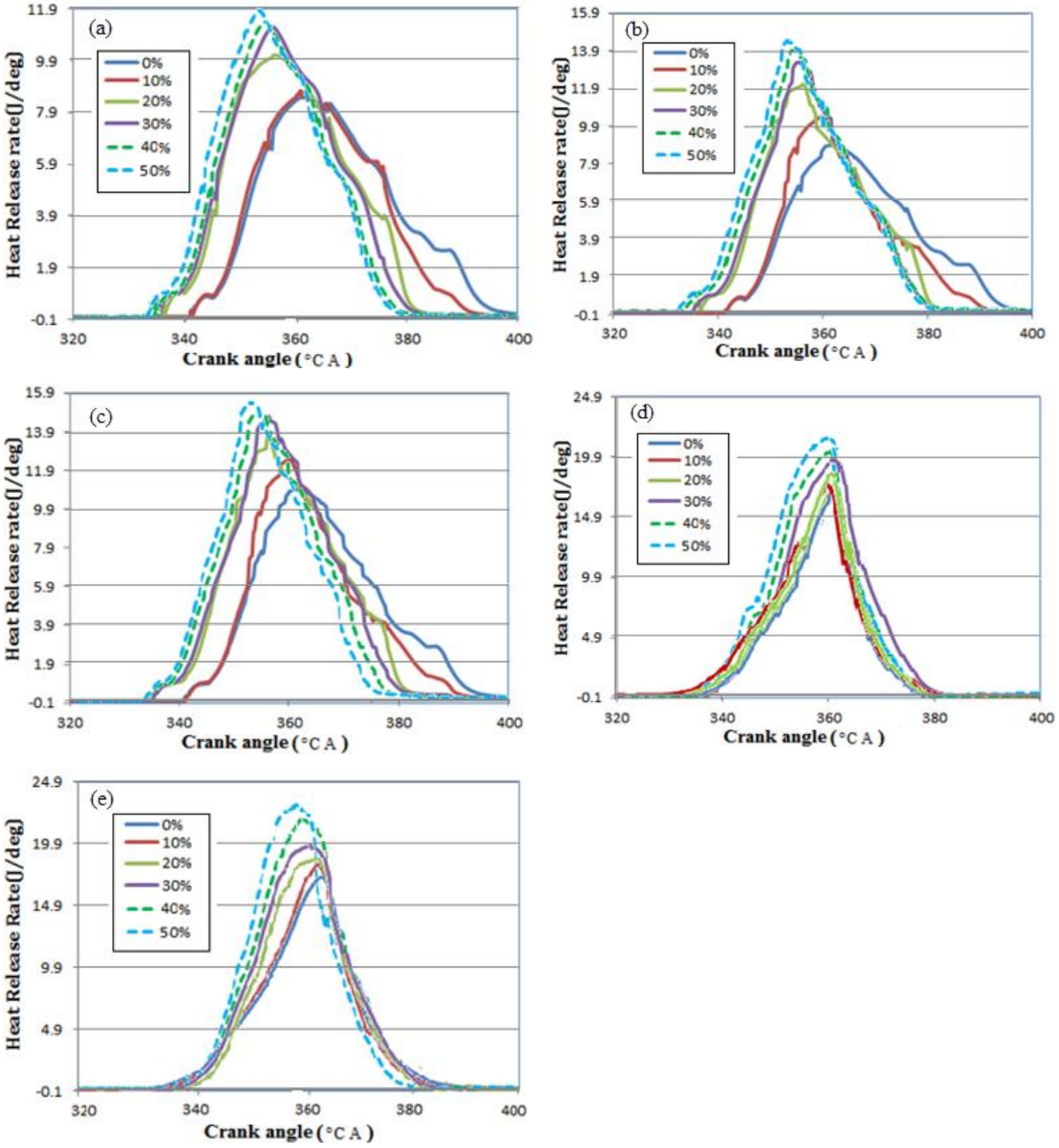

Fig. 7. Heat release rate versus the CA and spark timing of 19 °CA BTDC at 2000 rpm(a), 21 °CA BTDC at 3000 rpm (b), 23 °CA BTDC at 4000 rpm (c), 25 °CA BTDC at 5000 rpm (d), 28 °CA BTDC at 6000 rpm (e)

[DOI: 10.22068/ijae.8.1.2614]

7.2 Cumulative Heat Release

Mass fraction burned is the ratio of the cumulative heat release to the total heat release. Therefore if the mass fraction burned is known as a function of crank angle, then the apparent heat release can be approximated. The increase in cumulative heat release rate reduces the exhaust gas temperature in the engine pistons correspondingly improving the thermal efficiency of the engine. Figure 8(a) shows the comparison of the cumulative heat release rate at different engine speeds with natural gas fueled. In general, engine results show higher cumulative heat release rate at 6000 rpm ratio to lower speeds. The maximum difference was 774 J at 6000 rpm with 400 ^{o}CA. The increase in cumulative heat release rate reduces the exhaust gas temperature in the engine pistons correspondingly improving the thermal efficiency of the engine.

Figure 8(b, c, d, e, f) shows the effect of variations in the value of hydrogen percentage on cumulative heat release as a function of crank angle for HCNG fuel at different speeds. It can be seen that the hydrogen percentage has a very great effect on the magnitude and shape of the cumulative heat release curve. The highest value of the maximum cumulative heat release is obtained with HCNG 50% fuel. When comparing cumulative heat release between 2000 rpm up to 6000 rpm and that of 10% hydrogen in the blend and 50% hydrogen, it can be found that the sensitivity of cumulative heat release to changes in HCNG50% is higher than that for HCNG10%. The average cumulative heat release between cases HCNG10% up to HCNG50%, from 320 to 420 °CA is about 50 J. It implies that the sensitivity of the cumulative heat release curve to variations in the value of HCNG50% is higher than that for HCNG10%. By comparing the results obtained from 8 and 9, it is obvious that the effect of varying the engine speed on the trend of variation of the cumulative heat release curve and variation of the hydrogen percentage is similar.

7.3 Influence of mixtures of hydrogen and compressed natural gas on Power, Torque, Fuel Conversion Efficiency and Specific Fuel Consumption

The performance of the engine with respect to engine torque, power, and fuel conversion efficiency was investigated for CNG and 10%, 20%, 30%, 40%, and 50% Hydrogen was added to CNG fuel under steady state operations. Figures 9(a) and 9(b) present maximum power and torque of the engine at WOT versus various engine speeds form 2000 to 6000 rpm. The figure 10 and 11 shown that with rising of engine speed and percentage of hydrogen in the fuel blend, the maximum power and torque are increased and with more accurate looking to them, it can be observed that at low engine speed (2000 rpm), the maximum power for 0, 10, 20, 30, 40 and 50% hydrogen is 20.2, 20.91, 22.20, 22.38, 22.241 and 22.18 respectively. However, when the engine speed was run at 6000 rpm, the maximum power is 68.00, 69.2, 69.98, 70.012, 70.011 and 70.009. With an increase of hydrogen form 20% to up in the blend of fuel at 6000 rpm, the engine power is very low compared to 1.2% for changing 10% to 20% hydrogen in a blend. It was discovered that adding 20% hydrogen to fuel have yield better engine power as compared to 30%, 40%, and 50% hydrogen. In addition, adding a 20% amount of hydrogen can further enhance engine performance ratio to upper percentages. The description of this phenomena is due to the fact when the engine speed increases the combustion pressure have not thoroughly advanced due to the less available time for the mixing fuel and air that resulting in lower engine power [32]. Meanwhile, the maximum engine power obtained by CNG and blend of CNG and Hydrogen was about 68 and 70.012 kW, respectively, at 6000 rpm. With increasing hydrogen in the blend above 20%, a reduction power output was observed due to lower volumetric heating value [33].

Also, the curve of power has been plotted for different values of power output (kW) for 2000 and 6000 engine speed (rpm). Due to rapid combustion of hydrogen, a very little heat was lost to the environment and it burned many times faster than CNG air mixture. With the increase in the engine speed, the amount of power output also increased at a relative air to fuel ratio of a unit. The power output was found to be increasing due to the high calorific content of hydrogen.

Reduction of 1-11% power and torque with CNG operation was observed throughout the speed range. Maximum torque in this engine at 2000 rpm is equal 94.07 and 96.01 for CNG and 30% hydrogen. It can be seen that the maximum obtained torque was 102.31 and 104.2 Nm at 6000 rpm for CNG and HCNG20 blend fuel, respectively. But the maximum torque in this engine is at 4000 rpm and it is 108.35Nm and equal to 3.12% increase of torque. Varying the fuel composition from 20% hydrogen to upper has a result and it is that torque decrease from 104.2 to 103.21 at 6000 rpm. With goes engine speed up to 4000 rpm, engine torque increased and then decreased. Also in figures 10(a) and 10(b) can see a comparison between simulation data and experimental data by Wendy et al with CNG fuel only. Maximum 5% difference is visible between them [34]. So, we can say that the simulation results with experimental results have a good agreement.

[DOI: 10.22068/ijae.8.1.2614]

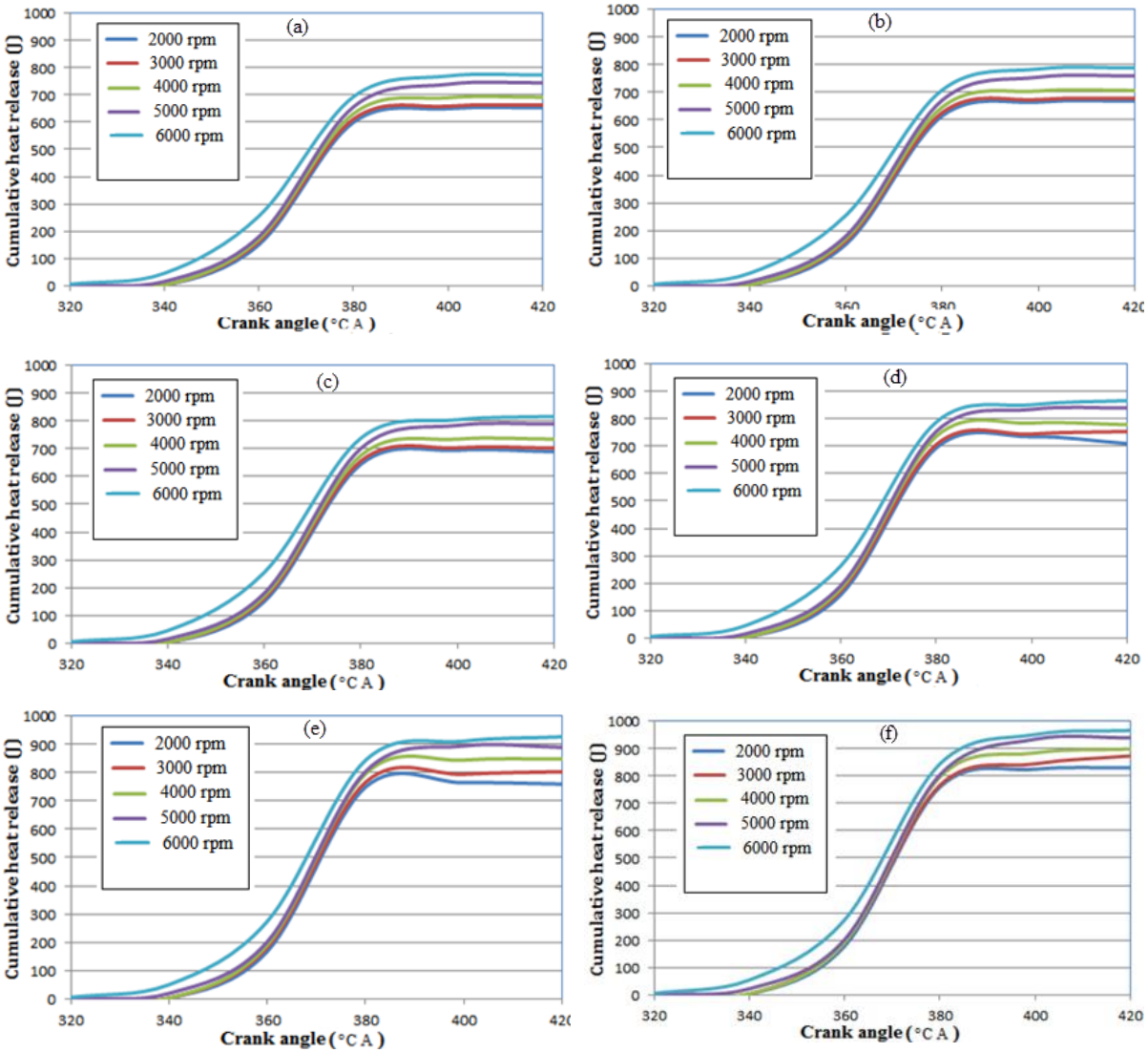

Fig. 8. Variation of cumulative heat release with crank angle at different speeds for CNG fuel (a), HCNG 10% fuel (b), HCNG 20% fuel (c), HCNG 30% fuel (d), HCNG 40% fuel (e), HCNG 50% fuel (f)

Fuel Conversion Efficiency may be an ideal way to measure efficiency. The Fuel Conversion Efficiency measurement begins with measuring the specific fuel consumption (sfc). This is the measure of mass fuel flow rate per unit power output. This measures how efficiently the engine is using the supplied fuel to do work: sfc is (mass fuel flow per unit time)/ (power output). There are, however, problems concerning sfc measurements in relation to the intention of the efficient-mileage rating system. There is no engine that runs at a constant speed at a constant load. Load and engine speed constantly change. As these change so does the sfc. A complete sfc measurement would result in a chart that looks like a topographical map. Measurements would need to be taken at many intervals of engine speed and many intervals of a given engine speed at an interval of the load. This would give a very detailed view of engine efficiency. Comparing relief maps of engine efficiency is only helpful to an engineer interested optimizing an engine's efficiency. Fuel Conversion Efficiency is ratio calculated from the sfc dimensional value. The Fuel Conversion Efficiency (nf) is the ratio of the engine output to the heating value of the fuel used (QHV) and nf = (Power)/(mass fuel flow rate x heating value of fuel).

[DOI: 10.22068/ijae.8.1.2614]

Figures below (Fig 12 and 13) show fuel conversion efficiency versus engine speed and percentage of hydrogen added to natural gas. Thermal efficiency has been previously called engine efficiency. However, the term fuel conversion efficiency is preferred because it describes this quantity more precisely and distinguishes it clearly from other definitions of engine efficiency. As we can see in the figure below with adding hydrogen to fuel and raise of engine speed, fuel conversion efficiency increased but its amount with varying the fuel composition form HCNG 20% to HCNG upper to 50% was insignificant. It was also found that CNG operation with direct injection achieved lower fuel conversion efficiency compared to HCNG engine. The results show by adding hydrogen to fuel, the fuel conversion efficiency has increased more than 3.7% due to enhancing the combustion event or improved combustion process and a decrease of unburned fuel in combustion chamber. Also, it proves that HCNG 20% is better for this engine because fuel conversion efficiency at 20% and 30% is near to each other and with increasing hydrogen to more than 20% we cannot see many changes. Therefore, hydrogen addition to the fuel (less than 30%) leads to significant efficiency increase. With the 30 vol.% HCNG fuel blend the highest efficiency is reached, while further increasing the hydrogen fraction in the fuel leads even to efficiency losses. The issue of the lower efficiency reached with the hydrogen richest fuel is worth of further scrutiny [35]. For drawing and calculation, Power and torque can use below formula. Thus, Engine Power and torque can be expressed as:

$$P = \frac{p_{cylinder} LAnK}{60 \times 1000} \quad (6)$$

,

$$T = \frac{p_{cylinder} LAn}{2\pi z} = \frac{p_{cylinder} \times V_e}{2\pi z}$$

Where: p = is cylinder pressure [N/m^2], A = cylinder area [m^2], L = stroke length [m], n = number of cylinders, z = 1 (for 2 stroke engines), 2 (for 4 stroke engines), V_e = engine swept volume [m^3]

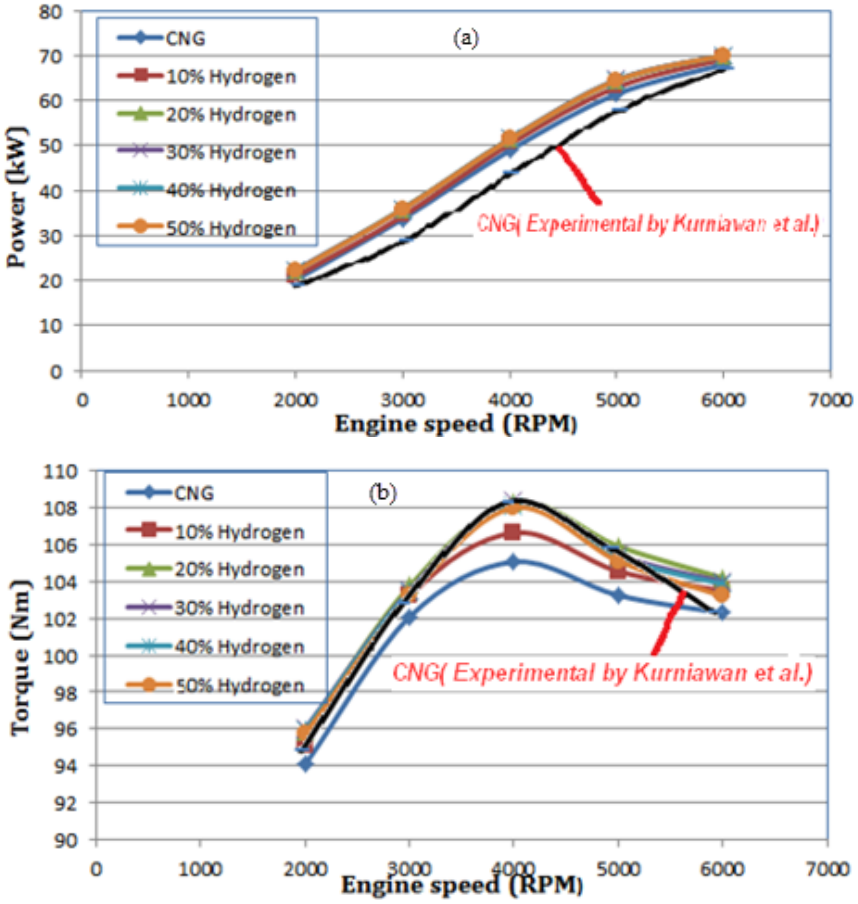

Fig. 9. Maximum powers versus engine speed (a), Maximum torques versus engine speed (b)

[DOI: 10.22068/ijae.8.1.2614]

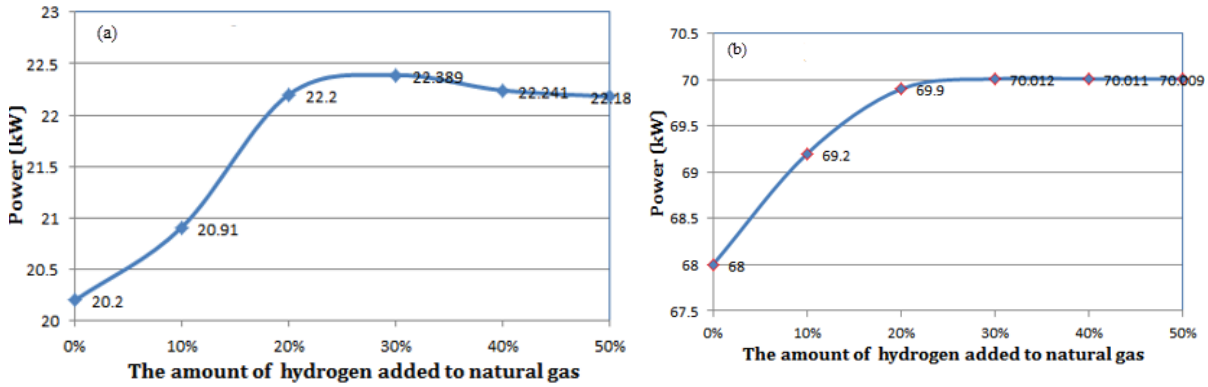

Fig. 10. Power versus the amount of hydrogen added to natural gas and spark timing of 19°CA BTDC at 2000 (a) and spark timing of 28°CA BTDC at 6000 rpm(b)

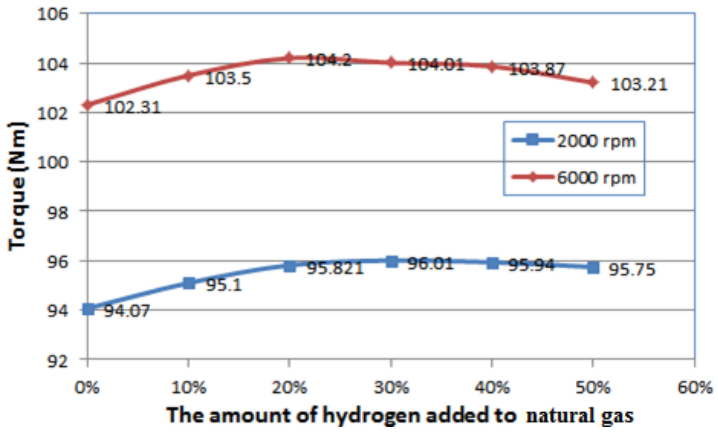

Fig. 11. Torque versus the amount of hydrogen added natural gas and spark timing of 19 °CA BTDC at 2000 and spark timing of 28 °CA BTDC at 6000 rpm

Specific fuel consumption, abbreviated SFC, compares the ratio of the fuel used by an engine to a certain force such as the amount of power the engine produces. It allows engines of all different sizes to be compared to see which is the most fuel efficient. It allows manufacturers to see which engine will use the least fuel while still producing a high amount of power. Figure 15 show the specific fuel consumption versus engine speed. As we can see at lower speeds, the SFC increases due to increased time for heat losses from gas to the cylinder and piston wall. While with increasing hydrogen to blend, specific fuel consumption is improved partially.

Figure 15(a, b, c, d, e) and 16 show, NO emission as a function of the engine speeds at 2000, 3000, 4000, 5000 and 6000 rpm. The increase of the engine speed resulted in the increase of NOx emissions and this is most probably due to the increase in combustion and cylinder temperature. NO Mass fraction (%) varies from 0.000208 at 2000rpm for CNG fuel to 0.004410 at 6000 rpm for HCNG 50%. The percentage of variation of NO in an engine (in this study) converted to HCNG fuel for 10%, 20%, 30%, 40% and 50% hydrogen obtained equal 50.75%, 427.7%, 887.37%, 901% and 932% respectively. A numerical study of a methane-fueled gas engine generator with the addition of hydrogen carried out by Park et al., shows that the NOx level for various hydrogen in the blend of fuel vary to 900% and its maximum obtained for 10 and 15% hydrogen [36]. The final result is that with respect to NO emissions, as the amount of hydrogen in the natural gas fuel increases, the NO emissions are reached for the high engine speed (6000 rpm).

[DOI: 10.22068/ijae.8.1.2614]

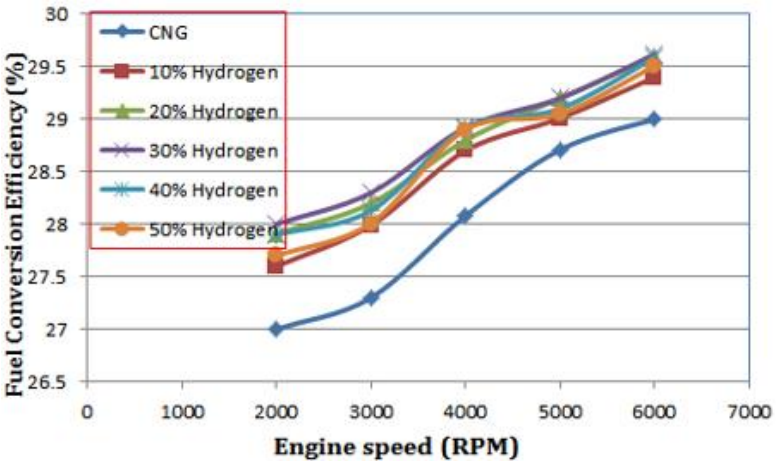

Fig. 12. Fuel conversion efficiency versus engine speed

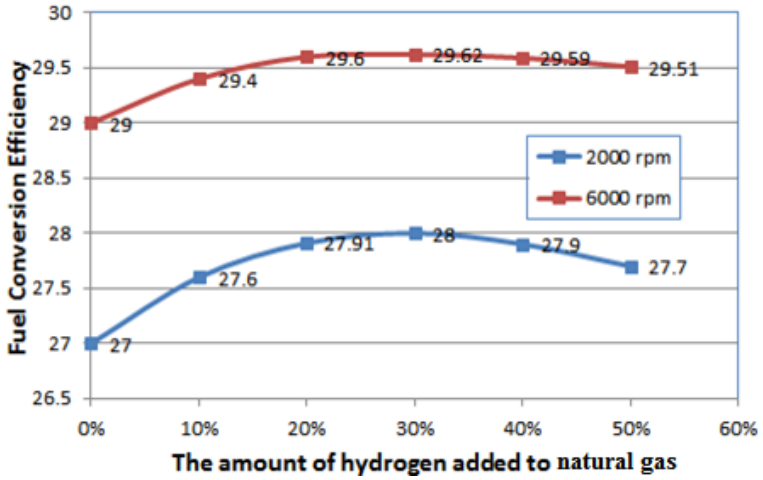

Fig. 13. Fuel conversion efficiency versus the amount of hydrogen added to natural gas and spark timing of 19 °CA BTDC at 2000 rpm and spark timing of 28 °CA BTDC at 6000 rpm

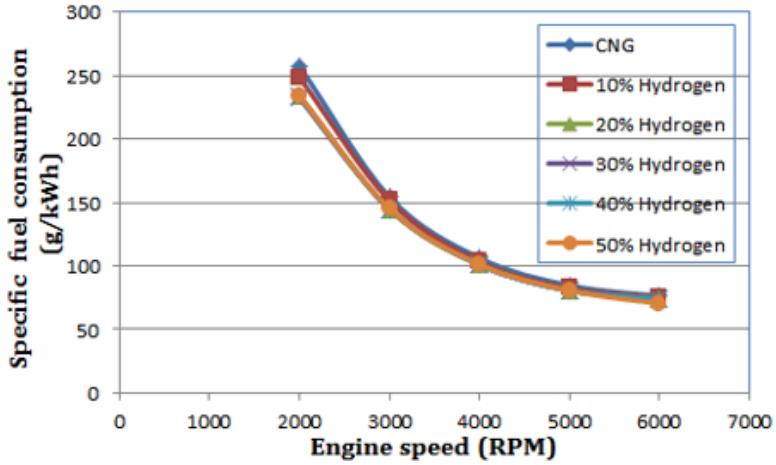

Fig. 14. Specific fuel consumption versus engine speed

[DOI: 10.22068/ijae.8.1.2614]

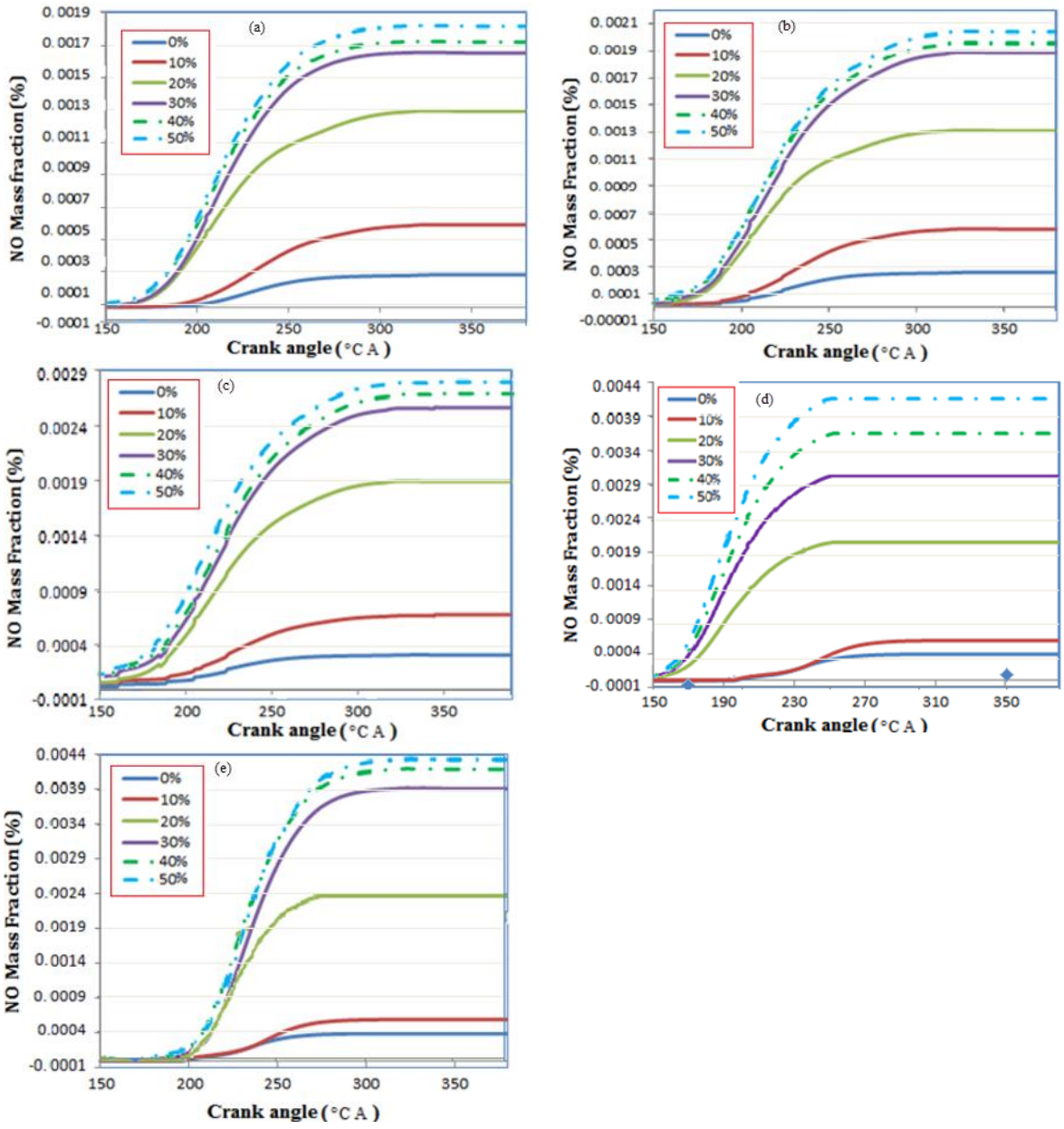

Fig15 .NO Mass fraction versus the CA at 2000 rpm (a), 3000 rpm (b), 4000 rpm (c), 5000 rpm (d), 6000 rpm (e)

[DOI: 10.22068/ijae.8.1.2614]

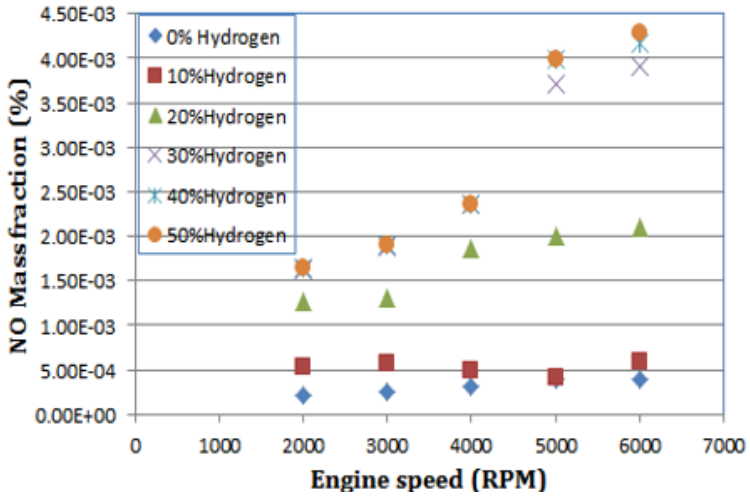

Fig. 16. NO emission as function of engine speed

8. CONCLUSION

Numerical results from others' works showed that the maximum in-cylinder pressure for hydrogen fuel was higher than the pure CNG due to hydrogen's fast combustion velocity. Also, it was expected that hydrogen- fueled engine must have zero CO emission. However, it was still present, which was due to burn of lubricant oil film inside the engine cylinder [37].

Although the hydrogen-fueled internal combustion engines have recently made significant progress, there are still major works need to be done to solve the above- mentioned problems. To increase the usage of alternative fuels while still using current technologies, the blending of hydrogen into natural gas fuel would be one of the options.

1-The results show that use of CNG fuel only in this engine have a positive performance in regarded to initiated map of ignition and injection timing due to maximum pressure and temperature happened after TDC.

2- With increasing hydrogen in the blend, increase of 3-11% of power, 1-4% of torque and 1-4% fuel conversion efficiency throughout the range of speeds with HCNG30% achieved but with adding hydrogen more than 30% to up, the performance began to decrease. Meanwhile, heat release rate increased with going up hydrogen in the blend but the duration of combustion became narrower due to high flame speed.

3- NOx due to the increase of temperature increased with increasing hydrogen in the blend but the lowest NOx was obtained at the lowest speed and retarded ignition timing, hence 19 degree BTDC.

References

[1]. Veziro T, Barbir F. Hydrogen: the wonder fuel. International Journal of Hydrogen Energy. 1992;17:391-404.

[2]. Kahraman E, Ozcanlı SC, Ozerdem B. An experimental study on performance and emission characteristics of a hydrogen fuelled spark ignition engine. International journal of hydrogen energy. 2007;32:2066-72.

[3]. Ji C, Wang S. Effect of hydrogen addition on lean burn performance of a spark-ignited gasoline engine at 800rpm and low loads. Fuel. 2011;90:1301-4.

[4]. Cacho JGL, Oliveros A, Barrera J. Development of a biogas fuel supply system for an internal combustion engine. Distributed Generation & Alternative Energy Journal. 2011;26:6-19.

[5]. Duc PM, Wattanavichien K. Study on biogas premixed charge diesel dual fuelled engine. Energy Conversion and Management. 2007;48:2286-308.

[6]. Wang T, Zhang X, Xu J, Zheng S, Hou X. Large-eddy simulation of flame-turbulence interaction in a spark ignition engine fueled with methane/hydrogen/carbon dioxide. Energy Conversion and Management. 2015;104:147-59.

[7]. Ma F, Wang Y, Liu H, Li Y, Wang J, Ding S. Effects of hydrogen addition on cycle-by-cycle variations in a lean burn natural gas spark-ignition engine. International Journal of Hydrogen Energy. 2008;33:823-31.

[DOI: 10.22068/ijae.8.1.2614]

[8]. Thurnheer T, Soltic P, Eggenschwiler PD. SI engine fuelled with gasoline, methane and methane/hydrogen blends: heat release and loss analysis. International Journal of Hydrogen Energy. 2009;34:2494-503.
[9]. Baratta M, d'Ambrosio S, Misul D, Spessa E. Effects of H2 addition to compressed natural gas blends on cycle-to-cycle and cylinder-to-cylinder combustion variation in a spark-ignition engine. Journal of Engineering for Gas Turbines and Power. 2014;136:051502.
[10]. Biffiger H, Soltic P. Effects of split port/direct injection of methane and hydrogen in a spark ignition engine. International Journal of Hydrogen Energy. 2015;40:1994-2003.
[11]. Morrone B, Unich A. Numerical investigation on the effects of natural gas and hydrogen blends on engine combustion. International journal of hydrogen energy. 2009;34:4626-34.
[12]. Yu X, Wu H, Du Y, Tang Y, Liu L, Niu R. Research on cycle-by-cycle variations of an SI engine with hydrogen direct injection under lean burn conditions. Applied Thermal Engineering. 2016;109:569-81.
[13]. Li H, Liu S, Liew C, Gatts T, Wayne S, Clark N, et al. An investigation of the combustion process of a heavy-duty dual fuel engine supplemented with natural gas or hydrogen. International Journal of Hydrogen Energy. 2017;42:3352-62.
[14]. Verma G, Prasad RK, Agarwal RA, Jain S, Agarwal AK. Experimental investigations of combustion, performance and emission characteristics of a hydrogen enriched natural gas fuelled prototype spark ignition engine. Fuel. 2016;178:209-17.
[15]. Xin Z, Jian X, Shizhuo Z, Xiaosen H, Jianhua L. The experimental study on cyclic variation in a spark ignited engine fueled with biogas and hydrogen blends. International Journal of Hydrogen Energy. 2013;38:11164-8.
[16]. Ghazal OH. A comparative evaluation of the performance of different fuel induction techniques for blends hydrogen–methane SI engine. International journal of hydrogen energy. 2013;38:6848-56.
[17]. Antunes JG, Mikalsen R, Roskilly A. An experimental study of a direct injection compression ignition hydrogen engine. International journal of hydrogen energy. 2009;34:6516-22.
[18]. Adnan R, Masjuki H, Mahlia T. Performance and emission analysis of hydrogen fueled compression ignition engine with variable water injection timing. Energy. 2012;43:416-26.
[19]. Alrazen HA, Talib AA, Adnan R, Ahmad K. A review of the effect of hydrogen addition on the performance and emissions of the compression–Ignition engine. Renewable and Sustainable Energy Reviews. 2016;54:785-96.
[20]. Zaker K, Askari MH, Jazayeri A, Ebrahimi R, Zaker B, Ashjaee M. Open cycle CFD investigation of SI engine fueled with hydrogen/methane blends using detailed kinetic mechanism. International Journal of Hydrogen Energy. 2015;40:14006-19.
[21]. Bauer C, Forest T. Effect of hydrogen addition on the performance of methane-fueled vehicles. Part I: effect on SI engine performance. International Journal of Hydrogen Energy. 2001;26:55-70.
[22]. Wong Y, Karim G. An analytical examination of the effects of hydrogen addition on cyclic variations in homogeneously charged compression–ignition engines. International Journal of Hydrogen Energy. 2000;25:1217-24.
[23]. Metghalchi M, Keck JC. Burning velocities of mixtures of air with methanol, isooctane, and indolene at high pressure and temperature. Combustion and flame. 1982;48:191-210.
[24]. Arthur D. Little Inc. Final report on an investigation of hazards associated with the storage and handling of liquid hydrogen. Report C-61092. 1960.
[25]. Tinaut F, Melgar A, Giménez B, Reyes M. Prediction of performance and emissions of an engine fuelled with natural gas/hydrogen blends. international journal of hydrogen energy. 2011;36:947-56.
[26]. Tinaut F, Melgar A, Giménez B, Reyes M. Characterization of the combustion of biomass producer gas in a constant volume combustion bomb. Fuel. 2010;89:724-31.
[27]. Eaton WW, Holzer CE, Von Korff M, Anthony JC, Helzer JE, George L, et al. The design of the Epidemiologic Catchment Area surveys: the control and measurement of error. Archives of general psychiatry. 1984;41:942-8.
[28]. Hogg RV, Ledolter J. Engineering statistics: Macmillan Pub Co; 1987.
[29]. Ma F, Wang Y, Liu H, Li Y, Wang J, Zhao S. Experimental study on thermal efficiency and emission characteristics of a lean burn hydrogen enriched natural gas engine. International Journal of Hydrogen Energy. 2007;32:5067-75.
[30]. Zeng K, Fu Y-X, Shi S, Wu C-I. Statistical tests for detecting positive selection by utilizing high-frequency variants. Genetics. 2006;174:1431-9.

[DOI: 10.22068/ijae.8.1.2614]

[31]. Ferguson C, Kirkpatrick A. Internal combustion engines applied thermosciences, John Wiley and Sons. Inc; 2001.

[32]. Wendy HK, Shahrir A, Kamaruzzaman S, Zulkifli MN, Azhari S. CFD investigation of fluid flow and turbulence field characteristics in a four-stroke automotive direct injection engine. 2008.

[33]. Dimopoulos P, Bach C, Soltic P, Boulouchos K. Hydrogen–natural gas blends fuelling passenger car engines: combustion, emissions and well-to-wheels assessment. International Journal of Hydrogen Energy. 2008;33:7224-36.

[34]. Park J, Cha H, Song S, Chun KM. A numerical study of a methane-fueled gas engine generator with addition of hydrogen using cycle simulation and DOE method. International journal of hydrogen energy. 2011;36:5153-62.

[35]. Patel C. Hydrogen Fueled IC Engine. International Journal of Hydrogen Energy. 2007;32:2066-72.

[DOI: 10.22068/ijae.8.1.2614]